Early antiviral CD4 and CD8 T cell responses are associated with upper respiratory tract clearance of SARS-CoV-2

Sydney I. Ramirez[1, 2], Paul G. Lopez[1], Farhoud Faraji[3], Urvi M. Parikh[4], Amy Heaps[4], Justin Ritz[5], Carlee Moser[5], Joseph J. Eron[6], David A. Wohl[7], Judith S. Currier[7], Eric S. Daar[8], Alex L. Greninger[9], Paul Klekotka[10], Alba Grifoni[1], Daniela Weiskopf[1,2], Alessandro Sette[1,2], Bjoern Peters[1,2], Michael D. Hughes[5], Kara W. Chew[7], Davey M. Smith[2†], and Shane Crotty[1,2†], for the ACTIV-2/A5401 Study Team

[1]Center for Vaccine Innovation, La Jolla Institute for Immunology, La Jolla, CA, USA
[2]University of California San Diego, Department of Medicine, Division of Infectious Diseases and Global Public Health, La Jolla, CA, USA
[3]University of California San Diego, Department of Otolaryngology-Head and Neck Surgery, La Jolla, CA, USA
[4]Division of Infectious Diseases, Department of Medicine, University of Pittsburgh School of Medicine, Pittsburgh, PA, USA
[5]Center for Biostatistics in AIDS Research, Harvard T.H. Chan School of Public Health, Boston, MA, USA
[6]Department of Medicine, University of North Carolina at Chapel Hill School of Medicine, Chapel Hill, NC, USA
[7]Division of Infectious Diseases, Department of Medicine, David Geffen School of Medicine at University of California, Los Angeles, Los Angeles, CA, USA
[8]Lundquist Institute at Harbor-UCLA Medical Center, Torrance, CA, USA
[9]Department of Laboratory Medicine and Pathology, University of Washington Medical Center, Seattle, WA, USA
[10]Eli Lilly and Company, San Diego, CA, USA

[†]Correspondence:
Shane Crotty, 9420 Athena Circle, La Jolla, CA, 92037, +1 858-752-6500, shane@lji.org;
Davey M. Smith, 9500 Gilman Drive #0679, La Jolla, CA, 92093, +1 858-642-1620, d13smith@health.ucsd.edu.

Running title: Early T cell responses to SARS-CoV-2 associated with upper airway viral clearance

ABSTRACT

T cells are involved in protective immunity against numerous viral infections. Limited data have been available regarding roles of human T cell responses controlling SARS-CoV-2 viral clearance in primary COVID-19. Here, we examined longitudinal SARS-CoV-2 upper respiratory tract viral RNA levels and early adaptive immune responses from 95 unvaccinated individuals with acute COVID-19. Acute SARS-CoV-2-specific CD4 and CD8 T cell responses were evaluated in addition to antibody responses. Most individuals with acute COVID-19 developed rapid SARS-CoV-2-specific T cell responses during infection, and both early CD4 T cell and CD8 T cell responses correlated with reduced upper respiratory tract SARS-CoV-2 viral RNA, independent of neutralizing antibody titers. Overall, our findings indicate a distinct protective role for SARS-CoV-2–specific T cells during acute COVID-19.

MAIN

Since the emergence of severe acute respiratory syndrome coronavirus 2 (SARS-CoV-2) as a novel human pathogen, much has needed to be learned about protective immunity to SARS-CoV-2 in the context of infection and COVID-19 vaccines. In the context of prophylaxis, both monoclonal antibodies and vaccine-elicited antibodies have demonstrated roles in protective immunity[1–6]. Serologic correlates of protection have been established for vaccines[7–14]. However, in the context of infection it is plausible that the relative importance of different compartments of the immune system shifts, and that viral control and clearance requires cellular immunity[15–19]. While there has been clear evidence of acute and memory T cell responses to SARS-CoV-2 infection[20–26] and COVID-19 vaccines[27–34], studies on protective roles of T cells have been limited in humans, particularly in non-hospitalized cases, given the technical difficulties of conducting large scale studies examining acute antigen-specific T cell responses and viral loads concomitantly in non-hospitalized individuals[19,35–37]. There is evidence for cellular immunity contributing to SARS-CoV-2 protection in non-human primate models[18]. Given expanded interest in next-generation COVID-19 and pan-sarbecovirus vaccines with T cell-specific components[38,39], or vaccines that are entirely T cell-based[32,40,41], future vaccine designs and clinical trial designs would benefit from better understanding of T cell protective immunity in humans.

We present longitudinal data for 95 individuals with primary SARS-CoV-2 infection prior to the availability of COVID-19 vaccines, with sampling including upper respiratory SARS-CoV-2 RNA levels and circulating SARS-CoV-2 neutralizing antibody, CD4 and CD8 T cell response measurements, all collected in the context of a clinical trial (ACTIV-2/A5401, NCT04518410), which is the largest and most comprehensive data set of its kind. All participants were enrolled within 7 days from positive SARS-CoV-2 testing and within 10 days from COVID-19 symptom onset. Participants were among those randomized to receive either 700 mg of the monoclonal antibody bamlanivimab or placebo (saline) intravenously on study day 0 (median of 6 days post-symptom onset; **Fig. S1A**). Peripheral blood was collected prior to treatment (study day 0) and on study days 7 and 28 for immunologic testing. We previously found that at day 28 nearly all of individuals tested had positive SARS-CoV-2-specific memory CD4 T cell responses, and a substantial fraction had memory CD8 T cell responses[23].

Here, we examined early SARS-CoV-2-specific CD4 and CD8 T cell responses and T cell response

kinetics during the acute phase of COVID-19 in the same 95 clinical trial subjects. We examined adaptive immune responses and associations with SARS-CoV-2 upper airway viral RNA in all 95 participants on study day 0 , in the absence of any treatment. Upper respiratory tract viral RNA and immune responses in persons who received bamlanivimab or placebo were considered together for study day 0, because swab and peripheral blood samples were collected prior to any treatment.Additionally, we examined longitudinal responses in the 49 participants in the placebo group. The 46 bamlanivimab treatment and 49 placebo subjects studied here were representative of the larger, overall clinical trial cohort of participants who were randomized to receive either 700 mg of bamlanivimab or placebo and were similar with respect to baseline characteristics such as age, sex at birth, risk for progression to severe COVID-19, and time post-symptom onset at randomization (**Table S1** and ref[23,42]).

Nasopharyngeal (NP) swabs were collected from all participants by trained study staff prior to treatment (on study day 0) and on study days 7, 14, and 28 to longitudinally measure SARS-CoV-2 RNA levels in the upper respiratory tract. As anticipated, ancestral SARS-CoV-2 viral RNA was detectable in the NP swabs of nearly all individuals (89%) at study day 0 (**Fig. 1A**). SARS-CoV-2 nasopharyngeal RNA levels did not differ between the bamlanivimab and placebo groups at study day 0 (**Fig. S1B**). SARS-CoV-2 NP RNA levels declined over time in the placebo group (**Fig. 1B**), as expected[43–45], and as previously reported for the complete ACTIV-2/A5401 clinical trial cohorts[42].

SARS-CoV-2 spike-specific and non-spike-specific CD4 T cells were measured by activation induced marker (AIM) assays following stimulation with spike and non-spike (CD4-RE[30]) peptide megapools (MP) (surface $OX40^+$ and $41BB^+$, **Fig. 1C and S1D**; surface $OX40^+$ and $CD40L^+$, **Fig. S1C and E.** See Methods). Virus-specific CD4 T cells were also assessed by combined AIM and intracellular cytokine staining (AIM+ICS), including interferon gamma production (IFNγ) (**Fig. 1D, S1F**). At study day 0, 85-87% of individuals had spike and non-spike (combined) SARS-CoV-2–specific CD4 T cell responses (**Fig. 1C-D, S1C-F**). Quantification of SARS-CoV-2-specific CD4 T cell frequencies was comparable by $OX40^+41BB^+$ or $OX40^+CD40L^+$ AIM (**Fig. 1C and S1C-E**). In parallel, SARS-CoV-2-specific CD8 T cell responses were evaluated by AIM+ICS (surface $CD69^+$ and intracellular $IFN\gamma^+$) following stimulation with SARS-CoV-2 spike and non-spike (CD8-RE[30]) MPs. 62% of individuals had detectable acute SARS-CoV-2–specific CD8 T cell responses at study day 0 (**Fig. 1E, S1G**). AIM^+ SARS-CoV-2-specific CD4 T cell frequencies and the number of positive responders increased over time (**Fig 1F, S1H**), while SARS-CoV-2-specific CD4 and CD8 T cell $IFN\gamma^+$ frequencies remained stable during the study period (**Fig 1G-H**). No differences were observed in SARS-CoV-2-specific CD4 and CD8 T cell frequencies between the bamlanivimab and placebo groups at study day 0, as expected (**Fig. S1D-G**). A positive correlation was observed between CD4 and CD8 T cell responses (**Fig. S2G-I**). Overall, acute virus-specific CD4 and CD8 T cell responses were detected in a substantial proportion of SARS-CoV-2–infected individuals at study day 0. Circulating follicular helper T cell responses (cT_{FH}) were also assessed by AIM assays, with similar response rates as seen for total antigen-specific CD4 T cells by AIM (**Fig. S1M-P**).

SARS-CoV-2 serologic assessments included neutralizing antibody (nAb) titers to ancestral SARS-CoV-2 by lentiviral pseudovirus neutralization assays (PSV NT50), and binding IgG antibody titers to the ancestral SARS-CoV-2 spike receptor binding domain (RBD) on study day 0, prior to treatment (**Fig. 1I-J and S1I-L**)[23]. Nab titers were detectable in 62% of individuals at study day 0 (**Fig. 1I**). As expected, endogenous nAb and RBD IgG titers increased in the placebo group between days 0 and 7 (**Fig. S1K-L**)

and a positive correlation was observed between day 0 nAb and RBD IgG titers (**Fig. S2F**).

To evaluate potential protective activities of early adaptive immune responses, associations were examined between NP viral RNA levels and SARS-CoV-2–specific immune responses. Early CD4 T cell responses measured at study day 0 were associated with lower levels of SARS-CoV-2 NP RNA based on all three main CD4 T cell measurements (Spearman r=-0.45, p=9.5x10^{-6} for AIM^+ by $OX40^+41BB^+$ **Fig. 2A, S2A**; r=-0.41, p=5.4X10^{-5} for AIM^+ by $OX40^+CD40L^+$, **Fig. S2D-E**; r=-0.37, p=4x10^{-5} for $AIM+ICS^+$, **Fig. 2B, S2B**). Early positive CD8 T cell responses were also associated with lower levels of SARS-CoV-2 NP RNA (r=-0.44, p=1.2x10^{-5}; **Fig. 2C, S2C**). The associations between SARS-CoV-2 NP RNA levels and T cell responses were strongest when combined AIM or AIM+ICS responses were considered but generally similar in magnitude and direction when spike and non-spike responses were evaluated separately (**Fig. S2J-Q** for total antigen-specific CD4 and for CD8 T cells**; S1R-Y** for antigen-specific cT_{FH}). Early nAb titers measured at study day 0 were also associated with lower levels of SARS-CoV-2 NP RNA (**Fig. 2D**), but less so than either the CD4 or CD8 T cell responses (r=-0.33, p=0.0012). Analysis of covariance (ANCOVA) testing was performed to better evaluate if the putative protective relationships observed between CD4 T cells or CD8 T cells and SARS-CoV-2 NP RNA remained after accounting for day 0 nAb seropositivity. The associations between CD4 T cells and SARS-CoV-2 viral loads or CD8 T cells and SARS-CoV-2 viral loads did not show a dependence on nAb seropositivity (**Fig. S2A-C, E**). Thus, both early SARS-CoV-2–specific CD4 and CD8 T cell responses are associated with reduced viral loads in unvaccinated non-hospitalized cases of acute COVID-19.

Participants in the study enrolled at a range of days post-symptom onset, which provides richness to the dataset, but raised the possibility that the immune response associations with reduced NP viral RNA levels might only be surrogates for days post-symptom onset. To test this possibility, an analysis was performed modeling T cell responses and NP viral RNA levels adjusted to account for time post-symptom onset, using a log-linear regression model of the raw data (**Fig. S3A**). If the original T cell associations with reduction of viral RNA levels were only surrogates of days PSO, T cell associations should be lost upon adjustment for days PSO. If instead the T cell associations reflected a functional relationship, statistical associations between T cell responses and lower viral RNA would be expected to improve. After accounting for days PSO, the relationships between T cell responses and reduced viral RNA levels were substantially stronger (CD4 AIM r =-0.66, p=1.1x10^{-12}. CD4 AIM+ICS r=-0.58, p=2.9x10^{-9}. CD8 AIM+ICS r=-0.58, p=1.8x10^{-9}. **Fig. 2F-G**), consistent with a functional role for T cells in control of NP viral RNA levels. Associations between nAb titers and viral RNA levels also improved, though still weaker than for CD4 or CD8 T cell responses (r=-0.48, p=2.1x10^{-6} **Fig. 2H**). Furthermore, if the model excluded the five individuals who tested negative for SARS-CoV-2 at study entry, the T cell associations with viral loads improved to r= -0.72 to -0.80 with p=6.3 x 10^{-15} to 8.0 x 10^{-20} (**Fig. S3B-E**); further evidence of functional relationships between the speed of acute CD4 and CD8 T cell responses in humans and control of SARS-CoV-2 NP viral loads.

In summary, it has been hypothesized that SARS-CoV-2–specific antiviral T cell responses may be protective due to enhanced viral clearance and reduced viral burden; however, few human studies have directly measured the role of cellular immunity on viral control, and with relatively small sample sizes[19,36,37]. Here, using peripheral blood and NP samples from close to 100 individuals from a randomized clinical trial, which is the largest and most comprehensive data set of its kind, the data demonstrate that stronger

early CD4 and CD8 T cell responses correlate with lower viral RNA levels in the upper airways, and the correlations are stronger after accounting for time from COVID-19 symptom onset. Overall, these findings suggest that SARS-CoV-2–specific T cells play a role in protective immunity to SARS-CoV-2 during acute infection, and that next generation SARS-CoV-2 or pan-sarbecovirus vaccines may benefit from enhanced T cell responses.

Our study has limitations. It is intrinsically challenging to disentangle the roles of T cells from the roles of antibodies in combatting SARS-CoV-2 in humans[17,19,20]. The study was also underpowered to distinguish whether the CD4 and CD8 T cell responses were each independently associated with lower viral loads. Lastly, our findings may not be reflective of all individuals with acute COVID-19, including breakthrough infection or primary infection with SARS-CoV-2 variants not assessed in this study.

METHODS

Study Population and Trial

ACTIV-2/A5401 is an ongoing, multicenter phase 2/3 randomized controlled trial designed to evaluate the safety and antiviral and clinical efficacy of therapeutics for acute COVID-19 in non-hospitalized adults. Individuals in this study represent a subset of participants from ACTIV-2/A5401 who received a single intravenous dose of 700 mg of bamlanivimab or normal saline placebo (comparator control group) and had available clinical data (e.g., demographics, days post-symptom onset, risk for severe COVID-19; **Table S1** and ref[23,42]) and blood samples for immunologic testing. Samples from nearly half of the overall bamlanivimab 700 mg and comparator placebo groups were available for this study. Participants were from the United States and enrolled in ACTIV-2/A5401 between October-November 2020. At study entry, COVID-19 vaccines were not available to the general population in the United States and SARS-CoV-2 infections could be attributed to ancestral SARS-CoV-2 virus. The subjects in this study were comparable at study entry across treatment groups (Table S1 and ref[23,42]). Inclusion criteria for ACTIV-2/A5401 included adults 18 years or older with no more than 10 days of COVID-19 symptoms and documented SARS-CoV-2 infection by FDA-authorized antigen or molecular testing within seven days prior to study entry. Subjects were assigned to the bamlanivimab or placebo groups at a 1:1 ratio, and randomization was stratified by time from symptom onset (less than or ≥5 days post-symptom onset) and risk of progression to severe COVID-19 based on age (less than or ≥ 55 years old) and the presence or absence of pre-defined comorbid medical conditions (e.g., body mass index > 35kg/m^2, hypertension, diabetes)[42]. Additional information for ACTIV-2/A5401 is available at ClinicalTrials.gov (Identifier: NCT04518410) and in the primary outcomes manuscript[42]. Three individuals were noted to have high NP viral loads despite high nAb titers at study day 0 (**Fig. 2D**). Notably, one of these three individuals was in the placebo group. It was subsequently re-confirmed that blood was drawn for all participants prior to bamlanivimab or placebo infusion, and that none of the placebo group participants received bamlanivimab or any other active drug treatment for COVID-19.

Partial data for day 0 RBD IgG titers by group, similar to the data shown in Fig S1I but with smaller sample sizes and without using a strict mean fluorescence intensity (MFI)-based cutoff, was previously published[23]. Although combined day 28 AIM and AIM+ICS data was published to show T cell response rates between the treatment and placebo groups[23], it was not presented as longitudinal data (as shown in Fig. 1F-H, S1G). Day 0 and 7 T cell data have not been published.

SARS-CoV-2 Viral RNA

Samples were collected, processed, and analyzed as previously reported[42]. In brief, nasopharyngeal swab samples were collected by ACTIV-2/A5401 trial staff at designated study sites on assigned study days (days 0, 7, 14, and 28) using standardized swabs and validated collection and storage procedures. nasopharyngeal swabs were frozen upon collection and stored at −80 °C (−65 °C to −95 °C) until shipped on dry ice to a central laboratory (University of Washington) for extraction, amplification and quantitative detection testing using validated, previously published methods using the Abbott m2000sp/rt system with a validated controls and standards for correlation with cycle threshold (Ct) and viral load. The limit of detection (LOD) was 1.4 log10 copies/mL, lower limit of quantification (LLOQ) was 2 log10 copies/mL, and upper limit of quantification (ULOQ) was 7 log10 copies/mL for this assay. For samples with viral RNA

levels above the ULOQ, samples were diluted, and the assay repeated to obtain a quantitative value.

PBMC and viability-based quality control

Peripheral blood was collected by ACTIV-2/A5401 trial staff at designated study sites on assigned study days. Serum and peripheral blood mononuclear cells (PBMC) for immunologic testing were isolated from whole blood using standard operating procedures. PBMC were cryopreserved and stored in liquid nitrogen until ready for use, then thawed at 37°C, resuspended in warm complete RPMI medium with 5% human AB serum (Gemini Bioproducts) and benzonase and centrifuged to remove cryopreservation medium. Following washing, cell counts were performed, and viability assessed using the Muse Count & Viability Kit (Muse Cell Analyzer; Luminex). A PBMC viability threshold was set at ≥ 75% for all samples for inclusion in data analysis. PBMC with viability below this threshold failed to appropriately respond to control stimuli. Four of 95 PBMC samples failed to meet the viability cutoff and were excluded from analyses. PBMC were resuspended to achieve a final concentration of 100,000 PBMC/100 µL for plating in 96-well format for T cell assays. Cryopreserved convalescent COVID-19 donor PBMC from known positive responders obtained from the Sette lab under an LJI IRB-approved protocol (VD-214) served as batch controls across T cell assays. These PBMC were handled in the same fashion as ACTIV-2/A5401 PBMC samples. Additional quality control metrics were also applied, as described below for the individual T cell assays.

Activation induced marker assay (AIM)

As previously described[23], PBMC were cultured for 24 hours at 37°C in an incubator with 5% CO_2 in the presence of negative control (equimolar amount of DMSO vehicle), positive control (Staphylococcal enterotoxin B at 1 µg/mL), or SARS-CoV-2 MPs (1 µg/mL per MP) [22,30,46] containing spike (S) [22,46] or non-spike epitopes (CD4-RE dominant and subdominant MPs) [30]. The spike MP was comprised of overlapping peptides spanning the full-length ancestral spike protein. The CD4-RE pool ("non-spike") consisted of experimentally validated class II epitopes from the remainder of the SARS-CoV-2 proteome.

PBMC were plated in 96-well plates with 1 x 10^6 PBMC per MP stimulation well and between 0.5-1 x 10^6 PBMC per control well; negative controls were plated in duplicate. Prior to stimulation, PBMC were incubated at 37°C for 15 minutes with 0.5 µg/mL anti-human CD40 mAb blocking antibody (Miltenyi Biotec). Chemokine receptor antibodies were also added on day 1 (see ref[23] for antibodies used in the AIM assay). After a 24-hour incubation, the plates were centrifuged, cells washed with PBS, then stained with LIVE/DEAD Fixable Blue (Invitrogen) 1:1000 in PBS with Fc block (5 µL/sample; BD Biosciences (BD)) for 15 minutes at room temperature, washed with FACS buffer (3% FBS in DPBS without calcium or magnesium), surface stained (see ref[23] for surface staining panel; 30 minutes at 4°C), fixed with BD Cytofix Fixation Buffer (4°C for 20 minutes), and stored at 4°C (up to overnight) until flow cytometric analysis was performed using a 5-laser Cytek Aurora (Cytek Biosciences). Analysis was performed using FlowJo (BD), and AIM^+ gates were drawn based on MP-stimulated responses relative to negative control.

PBMC quality was evaluated by measuring the median response to SEB for all samples, and samples with responses <50% of the overall median SEB response were excluded from downstream analyses. Two DMSO negative control well replicates were run for each sample and the average of the individual DMSO wells for each sample was calculated. T cell responses were verified by stimulation index

(SI) as a quality control. SI was calculated for each sample as the fold change in AIM^+ responses to MP-stimulation versus the average response to DMSO for the same subject. An SI cutoff of 2 was used for AIM^+ CD4 T cell responses; samples with an SI <2 were excluded from analysis of background subtracted AIM responses. When a non-zero DMSO value was needed for calculating the stimulation index, the minimum DMSO signal was set to 0.005%. For each MP-stimulated sample, the average DMSO value was subtracted from the MP response to calculate the background subtracted MP response. Combined AIM responses were calculated as the sum of the background subtracted responses to individual (spike and CD4-RE) MPs. In the case of negative AIM responses to both spike and CD4-RE megapools, the combined AIM response was also considered negative. The geometric mean of all DMSO negative control wells for each assay was calculated to determine the lower limit of quantitation (LOQ) for the assay. Positive responders were defined as those with background subtracted responses greater than the LOQ. The baseline for the y-axis was also set to 0.5 x LOQ or the closest log10 value. All non-responders were set at baseline.

Hybrid activation induced marker plus intracellular cytokine staining assay (AIM+ICS)

AIM+ICS assays were also performed as previously described[23]. PBMC were thawed and plated in parallel and as AIM assays but with the addition of wells for CD8-RE MP stimulation. The CD8-RE pool ("non-spike") consisted of experimentally validated class I epitopes from the remainder of the SARS-CoV-2 proteome. Cells were incubated with anti-CD40 blocking antibody as for AIM assays, but no chemokine receptor antibodies were added on day 1 except for CXCR5 for identification of cT_{FH} cells(see ref[23] for Ab used for AIM+ICS). After 20-22 hours, PMA (0.05 µg/mL) and ionomycin (0.25 µg/mL) were added to the positive (ICS) control wells. Two hours later, 0.25 µL/well of GolgiStop (BD) and GolgiPlug (BD) and the AIM marker Ab (see ref[23]) were added to all samples, and the plates were incubated for another 4 hours at 37°C (in a 5% CO_2 incubator). Cells were then washed, surface stained for 30 minutes at 4°C, fixed and washed using Cytofix/Cytoperm (BD) per the manufacturers' protocol. Intracellular cytokine staining was then performed using antibodies diluted in Perm/Wash Buffer (BD) for 30 minutes at 4°C. Cells were washed with Stain Buffer with FCS (BD) and stored in this buffer at 4°C until flow cytometric analysis was performed using a Cytek Aurora.

Gating and SI calculations were performed as described above for AIM assays. PMA + ionomycin served as an additional control for AIM+ICS assays for cytokine production (ICS). CD4 T cell responses with SI <2 and CD8 T cell responses with SI <3 were excluded from downstream analyses. For each MP-stimulated sample, the average DMSO value was subtracted from the MP response to calculate the background subtracted MP response. Combined AIM+ICS responses were calculated as the sum of the background subtracted responses to individual MPs (spike and CD4-RE for CD4 T cells, spike and CD8-RE for CD8 T cells). In the case of negative AIM+ICS responses to both spike and non-spike megapools, the combined AIM+ICS response was also considered negative. The LOQ and baseline was calculated as described above for AIM assays.

Binding antibody titers

Serum SARS-CoV-2-specific binding antibody assays were performed using the Bio-Plex Pro Human SARS-

CoV-2 IgG 4-Plex Panel serology assay (Bio-Rad 12014634) according to the manufacturer's protocol, as previously described[23]. MFI-based cutoffs for seropositivity are indicated in the figures.

Pseudovirus neutralizing antibody titers

Half-maximal neutralizing antibody titers (NT50) were generated using a lentiviral pseudovirus assay, as previously described[47]. Briefly, PSV was generated in HEK293T cells co-transfected with SARS-CoV-2 spike expression and pNL4–3.luc.R-E-mCherry-luciferase reporter packaging plasmids. Serum was isolated from the peripheral blood of study subjects using standard protocols, frozen and shipped to the testing site without thawing until ready for use. The serum was then serially diluted and incubated with SARS-CoV-2 PSV, then HEK293T cells stably expressing human angiotensin converting enzyme 2. Serum dilutions were run in triplicate. The percent inhibition was calculated using relative light units emitted by the reporter at each dilution and plotted versus the log serum dilution. The NT50 was then derived by non-linear regression. The limit of detection for the assay was defined by the lowest dilution tested (1:3) as indicated in figures.

Statistics

Statistical analyses were performed in GraphPad Prism 10 (GraphPad Software) and Microsoft Excel. Comparisons of SARS-CoV-2-specific T cell response magnitudes and antibody titers between treatment and placebo groups for equivalent conditions were determined by Mann-Whitney tests. Fisher's exact tests were used to compare SARS-CoV-2-specific T cell positive and negative response rates between treatment and control groups. Kruskal-Wallis nonparametric tests with post-hoc Dunn's multiple comparison tests were used for assessing T cell responses across more than one stimulation condition or cell type. Relationships between SARS-CoV-2 nasopharyngeal RNA levels and immune responses were assessed using nonparametric Spearman correlations.

Individual variation in days from symptom onset to study entry (day 0) was accounted for using a linear regression model. Adjusted SARS-CoV-2 NP RNA levels and adaptive immune responses (CD4 and CD8 T cell responses, nAb titers) at 6 days post-symptom onset (the median time from symptom onset at study entry) were calculated for all participants. For the viral RNA linear regression model, five day 0 NP RNA values were excluded as outliers. This included four values from individuals who consistently tested negative for viral RNA (nasal and NP) on all study days, and a value for one individual who tested negative on study day 0 but who subsequently tested positive (viral NP RNA positive on study days 3, 7, and 14). The adjusted NP viral RNA and adaptive immunity data, calculated for day 6 post-symptom onset, was then analyzed using nonparametric Spearman correlations, including all subjects (**Fig. 2E-H**). Additional correlation analyses were done excluding data from the five individuals with no detectable viral NP RNA at day 0 (**Fig. S3**). One-way ANCOVA were performed to control for the presence/absence of nAb on the relationships between SARS-CoV-2 NP RNA levels and Ag-specific T cell responses.

For all analyses, a two-sided 5% type I error rate was used, without adjustment for multiple comparisons, except as noted above. Additional details can be found in the results, figures and corresponding legends.

Study approval

The ACTIV-2/A5401 clinical trial protocol (ClinicalTrials.gov Identifier: NCT04518410) was approved by a central institutional review board (IRB); Advarra (Pro00045266). The La Jolla Institute for Immunology (LJI) IRB provided additional oversight for this study. All individuals enrolled in ACTIV-2/A5401 provided written informed consent for participation.

AUTHOR CONTRIBUTIONS

Conceptualization, S.I.R., D.M.S., and S.C.; Investigation, S.I.R., P.G.L., F.F., A.H.; Formal Analysis, S.I.R., B.P, S.C.; Patient Recruitment and Samples D.M.S.; Material Resources, A.G., D.W., P.K., A.S.; Writing, S.I.R., F.F., D.M.S. and S.C.; Supervision D.M.S. and S.C.

FUNDING

This work was supported in part by the National Institute of Allergy and Infectious diseases (NIAID) of the National Institutes of Health (NIH), Department of Health and Human Services, under contract no. 75N93019C00065 (A.S, D.W.), under awards AI036214, AI131385, UM1AI068634, UM1AI068636, and UM1AI106701. Additional support was provided in part by the John and Mary Tu Foundation, NIH T32 AI007036 (S.I.R.) and an A.P. Giannini Foundation fellowship award (S.I.R.). Bamlanivimab was donated by Eli Lilly and Company. The content presented is the sole responsibility of the authors and may not represent the opinions of the NIH.

ACKNOWLEDGMENTS

We would like to thank the study participants, site staff and investigators, members of the study team and community advisory board, the AIDS Clinical Trials Group (ACTG), the Harvard Center for Biostatistics in AIDS Research (CBAR) and ACTG Statistical and Data Analysis Center (SDAC), the National Institute of Allergy and Infectious Diseases (NIAID) / Division of AIDS (DAIDS), Bill Erhardt, the Accelerating COVID-19 Therapeutic Interventions and Vaccines (ACTIV) partnership, and PPD for making this study possible. See Supplemental Acknowledgments for additional details.

DATA AVAILABILITY

The authors confirm that the source data underlying the findings are fully available. Due to ethical restrictions, additional ACTIV-2/A5401 clinical trial study data beyond what is presented in this manuscript and supplement are available upon request from the AIDS Clinical Trials Group (ACTG) and with the written agreement of ACTG and the manufacturer of the investigational product. Completion of a data use agreement may be required.

COMPETING INTERESTS

S.I.R. has no competing interests to declare. J.S.C. has consulted for Merck and Company. A.L.G. reports contract testing from Abbott, Cepheid, Novavax, Pfizer, Janssen and Hologic and research support from Gilead, outside of the described work. P.K. is an employee and shareholder of Eli Lilly. D.W. is a consultant for Moderna. A.S. is a consultant for AstraZeneca Pharmaceuticals, Calyptus

Pharmaceuticals, Inc, Darwin Health, EmerVax, EUROIMMUN, F. Hoffman-La Roche Ltd, Fortress Biotech, Gilead Sciences, Gritstone Oncology, Guggenheim Securities, Moderna, Pfizer, RiverVest Venture Partners, and Turnstone Biologics. K.W.C. has received research funding to the institution from Merck Sharp & Dohme. D.M.S. has consulted for and has equity stake in Linear Therapies, Model Medicines and Vx Biosciences and consulted for Bayer, Kiadis, Signant Health and Brio Clinical. S.C. has consulted for GSK, JP Morgan, Citi, Morgan Stanley, Avalia NZ, Nutcracker Therapeutics, University of California, California State Universities, United Airlines, Adagio, and Roche. LJI has filed for patent protection for various aspects of T cell epitope and vaccine design work. The other authors have no competing interests to declare.

REFERENCES

1. Stadler, E. *et al.* Monoclonal antibody levels and protection from COVID-19. *Nat Commun* **14**, 4545 (2023).
2. Khoury, D. S. *et al.* Neutralizing antibody levels are highly predictive of immune protection from symptomatic SARS-CoV-2 infection. *Nat Med* **27**, 1205–1211 (2021).
3. Levin, M. J. *et al.* Intramuscular AZD7442 (Tixagevimab–Cilgavimab) for Prevention of Covid-19. *N Engl J Med* **386**, 2188–2200 (2022).
4. Isa, F. *et al.* Repeat subcutaneous administration of casirivimab and imdevimab in adults is well-tolerated and prevents the occurrence of COVID-19. *International Journal of Infectious Diseases* **122**, 585–592 (2022).
5. O'Brien, M. P. *et al.* Subcutaneous REGEN-COV Antibody Combination to Prevent Covid-19. *N Engl J Med* **385**, 1184–1195 (2021).
6. Cromer, D. *et al.* Predicting vaccine effectiveness against severe COVID-19 over time and against variants: a meta-analysis. *Nat Commun* **14**, 1633 (2023).
7. Gilbert, P. B. *et al.* Immune correlates analysis of the mRNA-1273 COVID-19 vaccine efficacy clinical trial. *Science* **375**, 43–50 (2022).
8. Corbett, K. S. *et al.* Immune correlates of protection by mRNA-1273 vaccine against SARS-CoV-2 in nonhuman primates. *Science* **373**, eabj0299 (2021).
9. Feng, S. *et al.* Correlates of protection against symptomatic and asymptomatic SARS-CoV-2 infection. *Nat Med* **27**, 2032–2040 (2021).
10. Gilbert, P. B. *et al.* A Covid-19 Milestone Attained — A Correlate of Protection for Vaccines. *N Engl J Med* **387**, 2203–2206 (2022).

11. Fong, Y. *et al.* Immune correlates analysis of the PREVENT-19 COVID-19 vaccine efficacy clinical trial. *Nat Commun* **14**, 331 (2023).

12. Fong, Y. *et al.* Immune correlates analysis of the ENSEMBLE single Ad26.COV2.S dose vaccine efficacy clinical trial. *Nat Microbiol* **7**, 1996–2010 (2022).

13. Regev-Yochay, G. *et al.* Correlates of protection against COVID-19 infection and intensity of symptomatic disease in vaccinated individuals exposed to SARS-CoV-2 in households in Israel (ICoFS): a prospective cohort study. *The Lancet Microbe* **4**, e309–e318 (2023).

14. Hertz, T. *et al.* Correlates of protection for booster doses of the SARS-CoV-2 vaccine BNT162b2. *Nat Commun* **14**, 4575 (2023).

15. Wilkinson, T. M. *et al.* Preexisting influenza-specific CD4+ T cells correlate with disease protection against influenza challenge in humans. *Nat Med* **18**, 274–280 (2012).

16. Sette, A. & Crotty, S. Adaptive immunity to SARS-CoV-2 and COVID-19. *Cell* **184**, 861–880 (2021).

17. Follmann, D. *et al.* Examining protective effects of SARS-CoV-2 neutralizing antibodies after vaccination or monoclonal antibody administration. *Nat Commun* **14**, 3605 (2023).

18. Goldblatt, D., Alter, G., Crotty, S. & Plotkin, S. A. Correlates of protection against SARS-CoV-2 infection and COVID-19 disease. *Immunol Rev* **310**, 6–26 (2022).

19. Sette, A., Sidney, J. & Crotty, S. T Cell Responses to SARS-CoV-2. *Annu. Rev. Immunol.* **41**, 343–373 (2023).

20. Rydyznski Moderbacher, C. *et al.* Antigen-Specific Adaptive Immunity to SARS-CoV-2 in Acute COVID-19 and Associations with Age and Disease Severity. *Cell* (2020) doi:10.1016/j.cell.2020.09.038.

21. Dan, J. M. *et al.* Immunological memory to SARS-CoV-2 assessed for up to 8 months after infection. *Science* **371**, (2021).

22. Grifoni, A. *et al.* Targets of T Cell Responses to SARS-CoV-2 Coronavirus in Humans with COVID-19 Disease and Unexposed Individuals. *Cell* **181**, 1489-1501.e15 (2020).

23. Ramirez, S. I. *et al.* Bamlanivimab therapy for acute COVID-19 does not blunt SARS-CoV-2–specific memory T cell responses. *JCI Insight* **7**, e163471 (2022).

24. Weiskopf, D. *et al.* Phenotype and kinetics of SARS-CoV-2–specific T cells in COVID-19 patients with acute respiratory distress syndrome. *Sci. Immunol.* **5**, eabd2071 (2020).

25. Notarbartolo, S. *et al.* Integrated longitudinal immunophenotypic, transcriptional and repertoire analyses delineate immune responses in COVID-19 patients. *Sci Immunol* **6**, eabg5021 (2021).

26. Gao, Y. *et al.* Ancestral SARS-CoV-2-specific T cells cross-recognize the Omicron variant. *Nat Med* **28**, 472–476 (2022).

27. Zhang, Z. *et al.* Humoral and cellular immune memory to four COVID-19 vaccines. *Cell* **185**, 2434-2451.e17 (2022).

28. Mateus, J. *et al.* Low-dose mRNA-1273 COVID-19 vaccine generates durable memory enhanced by cross-reactive T cells. *Science* **374**, eabj9853 (2021).

29. Rydyznski Moderbacher, C. *et al.* NVX-CoV2373 vaccination induces functional SARS-CoV-2-specific CD4+ and CD8+ T cell responses. *J Clin Invest* **132**, e160898 (2022).

30. Yu, E. D. *et al.* Development of a T cell-based immunodiagnostic system to effectively distinguish SARS-CoV-2 infection and COVID-19 vaccination status. *Cell Host & Microbe* **30**, 388-399.e3 (2022).

31. Tarke, A. *et al.* SARS-CoV-2 vaccination induces immunological T cell memory able to cross-recognize variants from Alpha to Omicron. *Cell* **185**, 847-859.e11 (2022).

32. Wherry, E. J. & Barouch, D. H. T cell immunity to COVID-19 vaccines. *Science* **377**, 821–822 (2022).

33. Sahin, U. *et al.* BNT162b2 vaccine induces neutralizing antibodies and poly-specific T cells in humans. *Nature* **595**, 572–577 (2021).

34. Müller, T. R. *et al.* Additive effects of booster mRNA vaccination and SARS-CoV-2 Omicron infection on T cell immunity across immunocompromised states. *Sci Transl Med* **15**, eadg9452 (2023).

35. Tan, A. T. *et al.* Early induction of functional SARS-CoV-2-specific T cells associates with rapid viral clearance and mild disease in COVID-19 patients. *Cell Reports* **34**, 108728 (2021).

36. Swadling, L. *et al.* Pre-existing polymerase-specific T cells expand in abortive seronegative SARS-CoV-2. *Nature* **601**, 110–117 (2022).

37. Lim, J. M. E. *et al.* SARS-CoV-2 breakthrough infection in vaccinees induces virus-specific nasal-resident CD8+ and CD4+ T cells of broad specificity. *J Exp Med* **219**, e20220780 (2022).

38. Arieta, C. M. *et al.* The T-cell-directed vaccine BNT162b4 encoding conserved non-spike antigens protects animals from severe SARS-CoV-2 infection. *Cell* **186**, 2392-2409.e21 (2023).

39. Tai, W. *et al.* An mRNA-based T-cell-inducing antigen strengthens COVID-19 vaccine against SARS-CoV-2 variants. *Nat Commun* **14**, 2962 (2023).

40. Sette, A. & Saphire, E. O. Inducing broad-based immunity against viruses with pandemic potential. *Immunity* **55**, 738–748 (2022).

41. Kingstad-Bakke, B. *et al.* Vaccine-induced systemic and mucosal T cell immunity to SARS-CoV-2 viral variants. *Proc. Natl. Acad. Sci. U.S.A.* **119**, e2118312119 (2022).

42. Chew, K. W. *et al.* Antiviral and clinical activity of bamlanivimab in a randomized trial of non-hospitalized adults with COVID-19. *Nat Commun* **13**, 4931 (2022).

43. Puhach, O., Meyer, B. & Eckerle, I. SARS-CoV-2 viral load and shedding kinetics. *Nat Rev Microbiol* (2022) doi:10.1038/s41579-022-00822-w.

44. Killingley, B. *et al.* Safety, tolerability and viral kinetics during SARS-CoV-2 human challenge in young adults. *Nat Med* **28**, 1031–1041 (2022).

45. Chen, P. *et al.* SARS-CoV-2 Neutralizing Antibody LY-CoV555 in Outpatients with Covid-19. *N Engl J Med* **384**, 229–237 (2021).

46. Grifoni, A. *et al.* SARS-CoV-2 human T cell epitopes: Adaptive immune response against COVID-19. *Cell Host and Microbe* **29**, 1076–1092 (2021).

47. Heaps, A. L. *et al.* Rapid determination of SARS-CoV-2 antibody neutralization titer using Bio-Rad Bio-Plex correlates strongly with pseudovirus-determined neutralization titer. *Journal of Virological Methods* **316**, 114726 (2023).

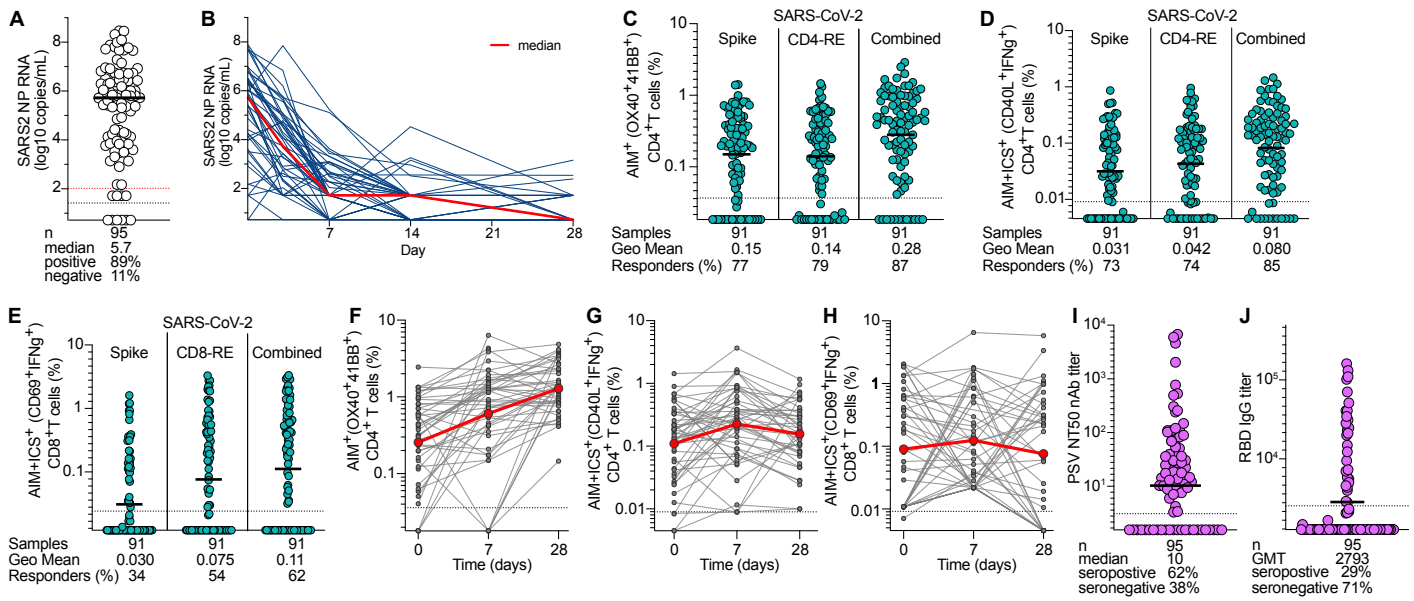

Figure 1. **SARS-CoV-2 NP RNA levels and adaptive immune responses in acute COVID-19**

A. SARS-CoV-2 NP RNA by quantitative reverse transcription polymerase chain reaction (RT-qPCR) for all participants prior to treatment on study day 0. Dotted black line limit of detection (LOD). Dotted red line limit of quantification (LOQ). Values >LOQ were considered positive. Bar = median. B. Longitudinal SARS-CoV-2 NP RNA data for the placebo group (n = 49) for days 0, 7, 14, and 28. Median for each time point in red. C. Day 0 CD4 AIM responses by surface OX40$^+$41BB$^+$. D. Day 0 CD4 AIM+ICS responses (by surface CD40L$^+$ and intracellular IFNγ$^+$). E. Day 0 CD8 AIM+ICS responses (by surface CD69$^+$ and intracellular IFNγ$^+$). For C-E: dotted black line indicates LOQ, bars represent geometric mean. F-H. Longitudinal combined AIM (F) and AIM+ICS (G, H) T cell responses in placebo group (n = 49) at days 0, 7, and 28. Red dots and lines represent median. I. Day 0 pre-treatment nAb titers. Dotted black line indicates LOD; seropositivity defined by values >LOD. Bar is median. J. Day 0 pre-treatment RBD IgG binding titers. Dotted black line indicates cut off for seropositivity. Bar is geometric mean titer (GMT).

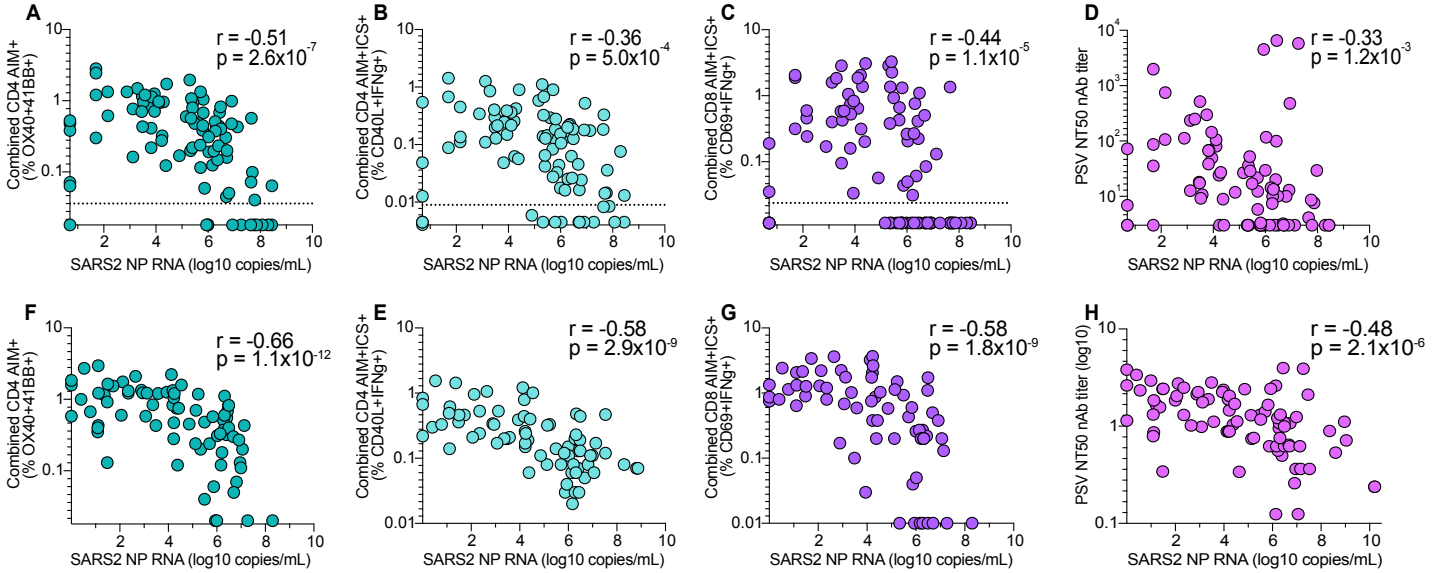

Figure 2. Correlative relationships between SARS-CoV-2-specific nAb and T cells and upper respiratory tract SARS-CoV-2 RNA levels. A-E. Correlation analysis of SARS-CoV-2 NP RNA and (A) CD4 AIM$^+$ (surface OX40$^+$41BB$^+$, as in Fig. 1C), (B) CD4 AIM+ICS$^+$ (surface CD40L$^+$ intracellular IFNγ^+, as in Fig. 1D), (C) CD8 AIM+ICS$^+$ (surface CD69$^+$ intracellular IFNγ^+, as Fig. 1E) T cell responses, and (D) nAb titers at study day 0. F-H. Correlation analyses as in E-H but adjusted for time from symptom onset. SARS-CoV-2 NP RNA and (E) CD4 AIM$^+$, (F) CD4 AIM+ICS$^+$, (G) CD8 AIM+ICS$^+$ T cell responses, and (H) nAb titers , all adjusted to day 6 post-symptom onset. All correlations by two-tailed nonparametric testing; r = Spearman's rank correlation coefficient.